PHYSICAL REVIEW A VOLUME 9, NUMBER 2 FEBRUARY 1974

Excitation-energy-dependent features in the continuum spectrum of cerium near the $M\alpha$ and $M\beta$ x-ray emission lines

M. B. Chamberlain
Air Force Materials Laboratory, Wright-Patterson Air Force Base, Ohio 45433

A. F. Burr and R. J. Liefeld
Department of Physics, New Mexico State University, Las Cruces, New Mexico 88001
(Received 10 September 1973)

M-series x-ray emission spectra from cerium have been recorded for near-threshold electron excitation. For incident electron energies near the M_{V} and M_{IV} inner-shell ionization energies, the spectra are dominated by intensity resonances of structures which are part of the continuous spectrum near its high-frequency limit. The intensity and position dependencies of the resonating structures are presented and are interpreted as arising from resonances in the cross sections for scattering electrons into empty $4f$ levels. No such resonances were observed for excitation energies near the M_{III} and M_{II} inner-shell ionization energies.

I. INTRODUCTION

The experimental results reported here show the dependence on incident electron energy of structures near the high-frequency limit of continuous x-ray spectra from cerium. Resonances in the intensity of this structure were observed for energies of incident electrons which were near the ionization energies of both the $M_{\mathrm{V}}(3d_{5/2})$ and the $M_{\mathrm{IV}}(3d_{3/2})$ inner-shell levels. The interpretation of these data is that this structure results from incident electrons being scattered into the available $4f$ valence levels with conversion of electron kinetic energy into single-photon energy. The fact that the observed structure exhibits intensity enhancement for certain energies of incident electrons is interpreted as evidence for resonances in the cross section for scattering incident electrons into these $4f$ levels. We explain the resonances as arising from sets of two-electron bound states involving a M_{V} or M_{IV} shell vacancy, the corresponding excited $3d$ electron, and the incident electron.

Experimental results showing the existence of similar resonant structures in the continuum spectra from lanthanum have been reported earlier.[1,2]

II. EXPERIMENTAL TECHNIQUES

The experimental procedure has been to record the intensity in the region of the high-energy limit of the continuous spectrum from a cerium anode x-ray tube for each of many values of the x-ray-tube voltage. The collected set of experimental curves displays the intensity of the x-ray radiation as a function of both the photon energy and the incident electron energy.

A. Sample preparation and instrumentation

A 99.9%-pure disk sample of cerium was placed in thermal contact with a water-cooled plate to form the anode of the x-ray tube. In order to reduce surface impurities, both the machining of the sample and the assembling of it into the x-ray tube were completed under a dry argon atmosphere. The x-ray-tube pressure was kept below 2×10^{-8} Torr during the acquisition of data. These steps provided for an essentially unoxidized cerium sample; in fact, the oxygen $K\alpha$ line was not detectable. The fluorine $K\alpha$ line was present, however, owing to the fact that the cerium was prepared by reduction of cerium fluoride. Its presence provided one of the several tests of the energy calibration of the spectrometer.

The two crystal vacuum spectrometer[3] used for the measurements actually operates as a variable energy monochromator. It utilized potassium acid phthalate crystals ($2d = 26.60$ Å) as the dispersing elements and a flowing gas proportional counter (90% argon and 10% methane at a pressure of 58 Torr) as the detector. Pulses from the counter were amplified, discriminated from the low-voltage noise, and stored with conventional electronics in a portion of the memory of a multichannel analyzer. Stored data were read out later onto punched paper tape for further analysis.

B. Standards and procedures

The voltage applied to the x-ray tube was monitored and maintained to within 10 mV of a constant value during the acquisition of each spectrum with the help of a voltage divider, a potentiometer, and a standard cell. The voltage recorded on each spectrum in the figures represents the potential difference between the Fermi levels of the metal sample and the metals which form the common ground of the electrical circuits. The absolute values of the anode voltages were measured with an accuracy of 100 ppm.

Spectrometer settings were placed on an absolute energy scale by following two steps. First, the absolute energy of the setting for the cerium $M\gamma$ line was assigned the energy given by Bearden and Burr.[4] Next, the energies of the remaining settings were calculated from the energy of the above setting by using the Bragg equation, the $2d$-spacing of the crystals, and the experimental observation that equal changes in the spectrometer settings effect, for all Bragg angles, corresponding equal changes in Bragg angle.

The intensity of each spectral distribution was determined by stepping the monochromator point by point through the spectrum with a dwell time at each point of 100 sec. Acquisition times for a complete spectrum ranged from 4 to 8 h.

The stability of the photon-counting apparatus was checked many times during the course of the experiments by recording the pulse height distribution of the x rays from a particular x-ray line, and comparing this with a reference distribution stored in another portion of the multichannel analyzer memory. The near threshold excitation conditions of the line, as well as the parameters associated with the proportional counter, the spectrometer settings and the counting electronics, were the same for each of these pulse-height distributions.

C. Data adjustments

The following three adjustments in the raw data were applied to the spectra which are reported here:

(i) A background of 18 counts/100 sec, which was obtained with the high voltage to the x-ray tube off, was subtracted from each data point.

(ii) The horizontal axis which was originally on a scale linear with the angle was converted to a scale linear with energy.

(iii) The number of counts at each data point was multiplied by a factor proportional to the reciprocal of the spectrometer transmission at that energy to effect an intensity scale independent of spectrometer setting. This adjustment was calculated from the coefficient of reflection of the first crystal, the percent reflection of the second crystal, the quantum counting efficiency of the proportional counter, and the transmission of the Formvar windows in the spectrometer. The experimental values for these variables have been published previously.[5,6]

III. EXPERIMENTAL RESULTS

The characteristics of the spectra obtained for cerium are very similar to the corresponding spectra previously reported for lanthanum.[2] For cerium, 70 spectra, each taken with a different anode voltage (between 674 and 1182 V) were recorded between x-ray energies of 660 and 1180 eV. Enough of the spectra are included here to illustrate the variations in structure which occur when the bombarding electrons have energies near the ionization energies of the M_V and M_{IV} levels.

Figure 1 shows a spectrum of the adjusted data points for the continuum radiation from the cerium target with an anode potential of 875.1 V, a voltage well below that necessary to excite the $M\alpha$ line (valence $\rightarrow M_V$). It has been shown[7,8] that the structure near the high frequency limit of such continuous spectra is dependent on the density of states available to electrons above the Fermi level; hence this linelike structure is termed the $4f$ structure in this case, because it corresponds to the large number of $4f$ levels available immediately above the Fermi level in cerium metal. It is the dependence of the size of this structure, which is emphasized by the crosshatching, upon the electron excitation energy that has been extensively studied in this experiment.

Figure 2 shows a number of spectra taken with bombarding electron energies near the threshold excitation energies of the M_V and M_{IV} levels. Column (a) shows a series of spectra taken as the anode voltage is increased (in 2-V steps) through the energy (882.5 eV) necessary to create M_V vacancies. The first frame shows a spectrum (on a reduced scale) very similar to that shown in Fig. 1. The second frame shows a spectrum created by electrons which have enough energy to excite the $M\alpha$ line. The $M\alpha$ line arises when

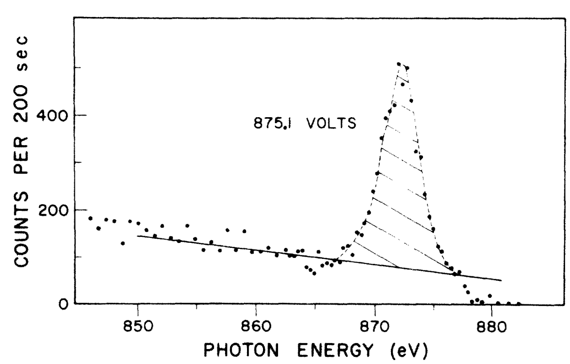

FIG. 1. Typical spectrum near the high-frequency limit of the continuum from cerium. The crosshatched area is used to construct Fig. 4 in the manner described in the text.

M_V vacancies are filled with $N_{VI,VII}$ electrons. Note that the intensity of the $4f$ structure has been greatly enhanced.

The next frame shows both the $M\alpha$ line and the $4f$ structure to be much more intense. The fourth frame shows the $4f$ structure completely overlapping the $M\alpha$ line and shows the intensity of both features to be reduced. In the fifth frame the intensities are further reduced and the $M\alpha$ line appears to be widened as the $4f$ structure starts to emerge from the high energy side of this line. In the last frame the $M\alpha$ line is reduced to a very low level and the $4f$ structure has virtually disappeared. (The small structure on the low-energy side of the $M\alpha$ line will be discussed later.)

Column (b) shows the corresponding spectra taken as the electron energy increases through the energy (898.7 eV) necessary to create M_{IV} vacancies. The first frame shows the $M\alpha$ line much the same as it was in the last frame. The $4f$ structure has recovered some of its intensity. In the second frame $M\beta$ photons are emitted as the M_{IV} vacancies are filled by N_{VI} electrons. The intensity of the $4f$ structure is again greatly

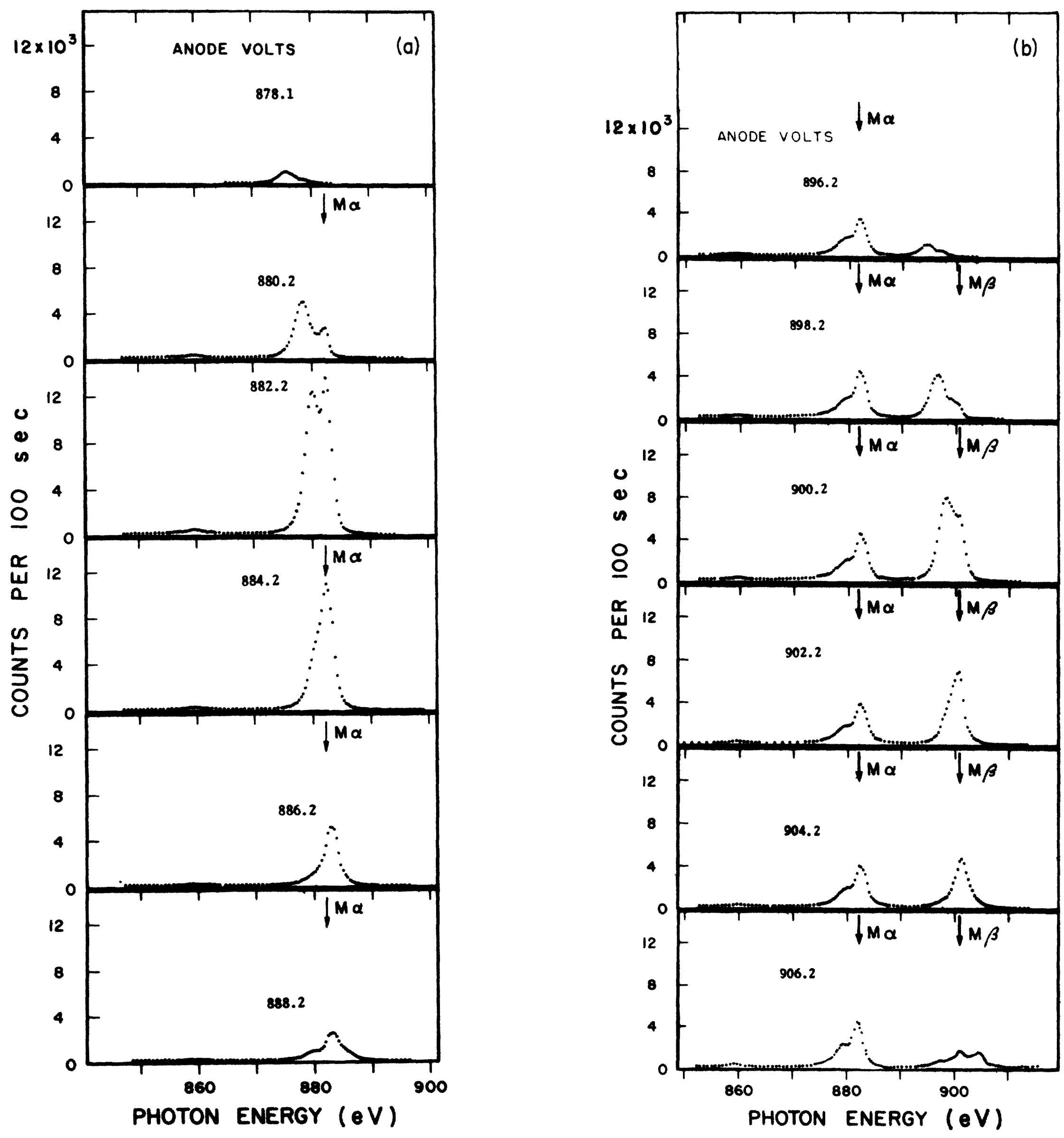

FIG. 2. Spectra of the type shown in Fig. 1 taken with bombarding electron energies near the threshold excitation energies of the M_V (column a) and M_{IV} (column b) levels.

increased. The third frame shows the process continuing. The two features overlap in the fourth frame with decreased intensity. The fifth frame shows the $M\beta$ line apparently widened as the $4f$ structure starts to emerge on the high-energy side. The last frame shows the $4f$ structure just resolved from the $M\beta$ line. This column of spectra also records changes in the intensity of the $M\alpha$ line due to the production of M_V level vacancies by Auger processes following M_{IV} vacancy production.

Figure 3 shows the entire region of interest with an anode voltage of 941.2 V, well above the voltage necessary to produce M_{IV} and M_V vacancies. The $4f$ structure at the extreme right is twice as intense as it was in Fig. 1. The $M\alpha$ and $M\beta$ lines are marked by arrows. On the low-energy side of each of these two characteristic lines are small structures which are discussed in the section on interpretation.

Figure 4 summarizes the intensity variations of the $4f$ structure as a function of the energy position of the peak of that structure. The intensity of the $4f$ structure was obtained by drawing a straight line through that part of the corrected continuous spectra beginning some 10 V from the high-frequency limit and extending to lower energies and taking as the intensity the area of the curve lying above this line extended toward the high-frequency limit. The area under discussion is illustrated by the crosshatched region in Fig. 1. The $M\alpha$ and $M\beta$ lines interfere with this direct measurement of intensity in the region where the $4f$ structures and the lines overlap. In these regions the intensity due to the lines and the intensity due to the $4f$ structure were separated by assuming both features to be symmetrical and estimating the area under the curve due to each. A dotted line is used in the curve in Fig. 4 for that small region where the overlap was so severe that the separation could not be made. The least value of the $4f$ structure intensity was assigned a value of 1 and occurred in the 868.1-eV spectrum, while its maximum value was 175 times larger and occurred in the 882.2 eV spectrum. The second maximum had a relative value of 105 and appeared in the 900.2-eV spectrum.

There are several notable features to the curve in Fig. 4. The most prominent are, of course, the two very large increases in intensity beginning just below the energy positions of the $M\alpha$ and $M\beta$ lines. The ratio of these two peaks is 5 : 3 and approximates the statistical weights of the M_V and M_{IV} levels. It is also interesting to note the variation in intensity of the $4f$ structure at other points on the graph. The intensity of the structure slowly decreased as the energy of the $M\alpha$ line was approached from below. It was very weak between the energies of the $M\alpha$ and $M\beta$ lines. This is the same general pattern as was found previously with a lanthanum target.[2]

IV. INTERPRETATION

The interpretation of the behavior of the spectra discussed in this paper and in the paper on lanthanum[2] is that the $4f$ structure is a portion of the continuous spectrum near the high-frequency limit which involves the scattering of incident electrons directly into the empty $4f$ levels just above the Fermi level. As mentioned previously the shape of the structure near the high-frequency limit approximates the density of states above the Fermi level. The principal additional feature presented by these experiments is the enhancement of this structure when the energy of the bombarding electrons is near that necessary to create a M_V or M_{IV} vacancy. The intensity resonances exhibited by the structure are explained as enhancements in the cross section for scattering incident electrons into the $4f$ levels via a mecha-

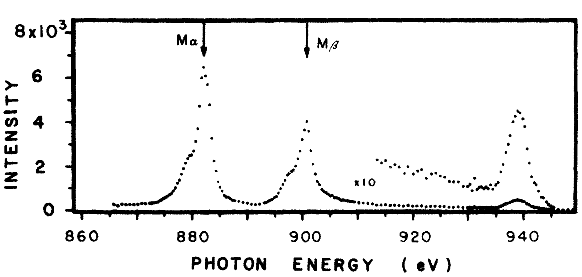

FIG. 3. Complete spectrum of the $M\alpha$ region showing the high-frequency limit on the right-hand side and with the $M\alpha$ and $M\beta$ characteristic lines labeled. The structures on the low-energy side of the lines are discussed in the text.

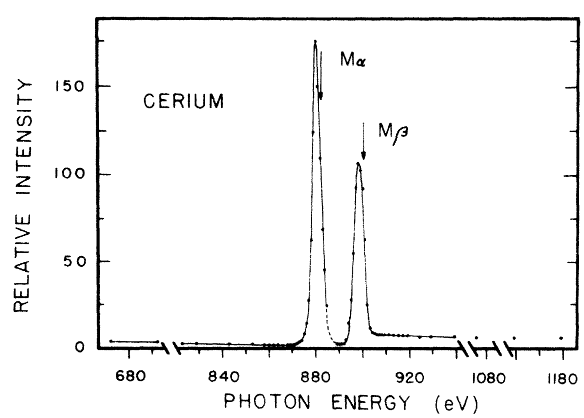

FIG. 4. Crosshatched area illustrated in Fig. 1 plotted vs the energy of the continuum peak. The graph shows the variation with energy of the cross section for production of continuum photons.

nism involving the incident electron, a cerium atom, and one of its inner shell electrons in a temporary negative-ion (bound-ejected-electron)[9] excited state. When this state decays radiatively to one in which the inner-shell vacancy is filled and the extra electron occupies one of the vacant $4f$ levels, the result is indistinguishable (by these experiments) from a process in which the incident electron is simply scattered into that $4f$ level with radiative loss of its original energy. The suggestion is that such atomic bound states provide the mechanism for enhancement of the electron-scattering cross section for certain limited ranges of incident electron energy near the ionization energies of particular inner shell levels. This suggestion also explains the small structures on the low energy side of the $M\alpha$ and $M\beta$ lines (see Fig. 3) when the exciting electrons have too much energy to be preferentially scattered into the $4f$ states. The structures are created by overly energetic electrons which have been slowed by inelastic scattering in the solid target to energies of about 900 and 882 eV, so that this resonant mechanism preferentially scatters them into the $4f$ levels with the emission of the appropriate photon. Of course, these overly energetic electrons are also inelastically scattered to other energies too; but for these energies there are no bound states which so strongly couple the electrons into the $4f$ levels.

Theoretical calculations and several observations from these experiments support the above interpretation. Wave-function calculations[10] show that in the lanthanide region of the periodic table the $4f$ wave functions strongly overlap the $3d$ wave function, thus providing a large spacial coupling between wave functions of these symmetries.

The observations that support this interpretation of the observations reported here include the fact that no resonances such as are shown in Fig. 4 occurred near the threshold for the creation of an M_{III} vacancy. Also note that the $M\alpha$ and $M\beta$ lines were only excited after the mechanism here had already increased the number of bombarding electrons scattering into the $4f$ states. Three other characteristic x-ray lines with the same initial state as the $M\alpha$ and $M\beta$ lines ($M_{\text{V}}O_{\text{III}}$, $M_{\text{V}}N_{\text{III}}$, $M_{\text{IV}}N_{\text{III}}$) appeared with the same excitation potential as those lines. Thus it is clear that the intermediate state exists only because of the corresponding $3d$ core vacancy and that the vacancy can be filled only by one of the bound-ejected-electrons returning to the $3d$ level and the other electron scattering into the vacant $4f$ state.

The outstanding feature of the electronic wave functions of the lanthanides, where the phenomenon reported here was first observed, is the large spacial overlap of the $3d$ and $4f$ wave functions. A further important point is that in this region of the periodic table it is the inner $4f$ shell which is being filled, after the $5s$, $6s$, $5p$, and even some $5d$ electrons already have been acquired. From these considerations one would expect to see related phenomenon in the transition metals where the $3d$ level is being filled and in the actinides where the $5f$ level is being filled. Indeed hindsight allows one to interpret a series of iron spectra made by Hanzely[11] as showing a continuum resonance decaying as the x-ray-tube voltage is varied through the energy necessary to create L_{III} vacancies.

ACKNOWLEDGMENTS

The support of the Research Corporation, the National Science Foundation, and the National Aeronautics and Space Administration made possible the development of the two-crystal x-ray spectrometer at New Mexico State University. One of us (M.B.C.) is indebted to the National Science Foundation for support through an NSF Graduate Traineeship during the course of this research. A grant from the Society of Sigma Xi also contributed to this program.

[1]A. F. Burr and R. J. Liefeld, in *Developments in Applied Spectroscopy*, edited by E. L. Grove and A. J. Perkins (Plenum, New York, 1969) p. 121.

[2]R. J. Liefeld, A. F. Burr, and M. B. Chamberlain, Phys. Rev. A 9, 316 (1974).

[3]R. J. Liefeld, in *Soft X-Ray Band Spectra*, edited by D. J. Fabian (Academic, New York, 1968), p. 133.

[4]J. A. Bearden and A. F. Burr, Rev. Mod. Phys. 39, 125 (1967).

[5]B. L. Henke, R. L. Elgin, R. E. Lent, and R. B. Ledingham, Norelco Reporter 14, 112 (1967).

[6]R. J. Liefeld, S. Hanzely, T. B. Kirby, and D. Mott, Adv. X-Ray Anal. 13, 373 (1970).

[7]K. Ulmer, in Proceedings of the International Symposium on X-Ray Spectra and Electronic Structure of the Substance, Kiev, U.S.S.R., 1966 (unpublished).

[8]R. R. Turtle and R. J. Liefeld, Phys. Rev. A 7, 3411 (1973).

[9]L. G. Parratt, Rev. Mod. Phys. 31, 616 (1959).

[10]F. Herman and S. Skillman, *Atomic Structure Calculations* (Prentice-Hall, Engelwood Cliffs, N. J., 1963).

[11]S. Hanzely and R. J. Liefeld, *An L-Series X-Ray Spectroscopic Study of the Valence Bands in Iron, Cobalt, Nickel, Copper and Zinc*, Natl. Bur. Std. (U. S.) (U. S. GPO, Washington, D. C., 1971).